



UNIVERSITY OF LEEDS

This is a repository copy of *Using Confinement to Study the Crystallisation Pathway of Calcium Carbonate*.

White Rose Research Online URL for this paper:  
<http://eprints.whiterose.ac.uk/123040/>

Version: Accepted Version

---

**Article:**

Wang, Y, Zeng, M [orcid.org/0000-0002-8627-4146](https://orcid.org/0000-0002-8627-4146), Meldrum, FC et al. (1 more author) (2017) Using Confinement to Study the Crystallisation Pathway of Calcium Carbonate. *Crystal Growth and Design*, 17 (12). pp. 6787-6792. ISSN 1528-7483

<https://doi.org/10.1021/acs.cgd.7b01359>

---

© 2017 American Chemical Society. This document is the Accepted Manuscript version of a Published Work that appeared in final form in *Crystal Growth and Design*, copyright © American Chemical Society after peer review and technical editing by the publisher. To access the final edited and published work see <https://doi.org/10.1021/acs.cgd.7b01359>

**Reuse**

Items deposited in White Rose Research Online are protected by copyright, with all rights reserved unless indicated otherwise. They may be downloaded and/or printed for private study, or other acts as permitted by national copyright laws. The publisher or other rights holders may allow further reproduction and re-use of the full text version. This is indicated by the licence information on the White Rose Research Online record for the item.

**Takedown**

If you consider content in White Rose Research Online to be in breach of UK law, please notify us by emailing [eprints@whiterose.ac.uk](mailto:eprints@whiterose.ac.uk) including the URL of the record and the reason for the withdrawal request.



[eprints@whiterose.ac.uk](mailto:eprints@whiterose.ac.uk)  
<https://eprints.whiterose.ac.uk/>

## Using Confinement to Study the Crystallisation Pathway of Calcium Carbonate

Yunwei Wang<sup>1</sup>, Muling Zeng<sup>2</sup>, Fiona C. Meldrum<sup>1\*</sup> and Hugo K. Christenson<sup>2\*</sup>

<sup>1</sup>School of Chemistry, <sup>2</sup>School of Physics and Astronomy, University of Leeds,  
Leeds, LS2 9JT, UK.

### ABSTRACT

Studies of crystallisation in small volumes have shown that constraining the space in which precipitation occurs can provide an effective means of studying the pathways by which crystallisation occurs. This article describes an investigation into the precipitation of calcium carbonate in a crossed-cylinder apparatus, where the confinement of low solution concentrations between unfunctionalised glass surfaces delivers a dramatic increase in the lifetime of metastable phases. This phenomenon allows the direct observation of amorphous calcium carbonate (ACC) in very dilute systems where it is virtually undetectable in bulk solution, thus confirming the predictions of a recent titration study which showed that the solubility product of ACC is an order of magnitude lower than previously believed. The aggregation of ACC particles is also seen to significantly decrease with increasing confinement, suggesting that the stability of ACC in confinement is related to its aggregation state and restricted mobility. Finally, we observe that ACC transforms to calcite via the metastable phase vaterite in constrained volumes at solution concentrations where direct transformation to calcite occurs in bulk solution. This work underscores the utility of using confinement to detect and preserve transient metastable phases in bulk solution, where this may have applications in materials syntheses utilising amorphous precursor phases.

## INTRODUCTION

There is currently widespread interest in crystallisation mechanisms, where it is now recognised that many minerals can form via processes including the oriented assembly of crystalline nanoparticles, or through intermediate amorphous phases.<sup>1</sup> Amorphous precursor phases have attracted particular attention for their importance as biominerals, and the significance of amorphous calcium carbonate (ACC) in the formation of calcite biominerals is now well established.<sup>2</sup> This has initiated a wide range of fundamental studies of ACC that have focussed on topics including the possible role of pre-nucleation clusters in its precipitation,<sup>3,4</sup> the relationship between short-range order in the amorphous phase and the structure of the product crystalline polymorphs,<sup>5,6,7,8,9</sup> and the mechanism of transformation of ACC.<sup>4,10-12</sup> Spinodal decomposition, or liquid-liquid phase separation, has been suggested as a route to ACC precipitation from metastable  $\text{CaCO}_3$  solutions of higher supersaturation,<sup>13,14</sup> whereas classical nucleation would occur at lower concentrations, below 3-4 mM.<sup>15</sup> The unique properties of ACC have also led to its use in fabricating devices and materials<sup>16</sup> such as microlens arrays,<sup>17</sup> composite polymeric materials,<sup>18</sup> nacre-inspired layered nanocomposites,<sup>19</sup> and porous single crystals of calcite.<sup>20</sup> Medical applications include drug delivery,<sup>21</sup> protein adsorption,<sup>22</sup> enhanced calcium delivery<sup>23</sup> and artificial bone scaffolding.<sup>24</sup>

One of the most fascinating features of ACC is the potential not only to control the rate at which it transforms, but also to define the structure and morphology of the product crystalline phase. This is beautifully illustrated by biomineralization processes, where transformation of transient ACC can lead to structures such as single crystals with complex morphologies.<sup>25</sup> A range of candidate biomacromolecules and inorganic ions have been implicated in the biogenic stabilisation of ACC, and have inspired the use of soluble additives<sup>26-29</sup> and organic matrices<sup>30,31</sup> to control

ACC crystallisation in synthetic systems. Interestingly, a number of recent studies have also suggested that confinement effects may play an important role in this process.<sup>32-37</sup> ACC usually precipitates homogeneously from a supersaturated solution, but within minutes the globular particles convert to calcite (or to vaterite at higher supersaturations), either at the surface of the particles, or indirectly, by nucleation elsewhere in the system.<sup>38</sup> In contrast, ACC can exhibit significantly extended lifetimes in confinement as compared to bulk solution.<sup>34,35</sup> The mechanism underlying this phenomenon is intriguing, where stabilisation of metastable phases has been observed for inorganic systems including calcium sulfate<sup>39</sup>, calcium oxalate,<sup>40</sup> calcium phosphate<sup>41,42</sup> and potassium ferrocyanide,<sup>43</sup> and more generally for a range of organic compounds.<sup>44</sup>

This article describes an investigation into the mechanism by which ACC transforms to crystalline calcium carbonate in confined volumes, where experiments were conducted using a crossed-cylinder apparatus in which the degree of confinement varies continuously from zero at the contact point between the glass cylinders to macroscopic dimensions. In previous experiments using this apparatus<sup>34</sup> the glass was functionalised with gold/ self-assembled monolayers (SAMs) of mercaptohexadecanoic acid (MHA) that promote the nucleation and growth of oriented calcite crystals<sup>45</sup> and employed 4 – 8 mM solutions. Under these conditions large masses of ACC were observed that transformed to calcite and the common kinetic polymorph vaterite was never observed. Using bare glass surfaces and solution concentrations down to 0.5 mM, we here demonstrate that ACC can be observed at concentrations of 0.5 mM, consistent with recent suggestions regarding the solubility product of ACC<sup>46</sup> and that it can transform to calcite via a vaterite intermediate. Importantly, our data also provide strong evidence that the rate of

transformation of ACC in confinement is related to its aggregation state, further contributing to our understanding of confinement effects on inorganic crystallisation.

## **EXPERIMENTAL**

**General Methods:**  $\text{CaCO}_3$  was precipitated at room temperature ( $T = 22 \pm 2 \text{ }^\circ\text{C}$ ) by the double-decomposition method from metastable solutions by mixing equal quantities of equimolar aqueous solutions (Milli-Q water, resistivity =  $18.2 \text{ M}\Omega \text{ cm}$ ) of  $\text{CaCl}_2 \cdot 2\text{H}_2\text{O}$  (pH = 6.0) and  $\text{Na}_2\text{CO}_3$  (pH = 11.4) (both Sigma-Aldrich). The glassware was cleaned in Piranha solution ( $\text{H}_2\text{SO}_4/\text{H}_2\text{O}_2$  4:1) overnight, then rinsed with de-ionised water and ethanol and finally dried with nitrogen gas. Solutions of concentrations  $[\text{Ca}^{2+}] = [\text{CO}_3^{2-}] = 0.5, 1.0, 1.5, 2.5$  and  $4.5 \text{ mM}$  were employed, where all experiments were repeated 10 times with the exception of the 2.5 and 4.5 mM solution which were repeated three times each.

**Control Experiments:**  $\text{CaCO}_3$  precipitates formed in bulk solution were collected on carbon/Formvar-coated Cu TEM grids (200 mesh) by immersing the grids in the crystallisation solution for 2 s, rinsing them with ethanol and drying at room temperature. Samples were collected after precipitation times ranging from 15 s to 24 h.

**Precipitation of Calcium Carbonate in Confinement:** Precipitation in confinement was carried out by placing a droplet (ca.  $50 \text{ }\mu\text{L}$ ) of solution around the contact point between the two crossed glass cylinders of equal radius,  $R = 5 \text{ cm}$ , or four times larger than in previous work. In order to be able to use electron diffraction to identify the polymorph of the precipitates, some experiments were carried out with Cu TEM grids sandwiched between the centres of the two crossed cylinders.

Each experiment was terminated, usually after 24 h, by separating the surfaces, and rapidly rinsing the glass cylinders with ethanol followed by air drying. When Cu grids were present, these were removed after separating the cylinders, rinsed carefully with ethanol and air dried. Precipitates were only occasionally analysed after longer times as we could not ensure that the solution concentration did not begin to increase due to evaporation.

In each experiment, the distance from the contact point  $x$  of positions on the glass cylinders between the cylinders was noted so that the approximate surface separation  $h$  at which the precipitates had been located could be determined according to<sup>34</sup>

$$h = R - \sqrt{R^2 - x^2} = x^2/2R \quad (1)$$

With the TEM grids, however, the surface separation cannot be determined in this manner since the configuration is that of a cylinder on a flat surface, and for a given radial distance  $x$  from contact the separation varies from 0 to  $h$ . Nevertheless, the use of electron diffraction allowed us to determine the polymorph of crystals that were morphologically similar to those in the SEM images, which were located at more accurately determined surface separations. Note that the crystals and ACC particles in confinement were too small ( $< 1 \mu\text{m}$ ) to enable the use of Raman microscopy, infrared spectroscopy or powder X-ray diffraction as a supporting identification techniques.

**Analysis:** The glass cylinders supporting calcium-carbonate particles were mounted on SEM stubs using conducting carbon tape and were sputter-coated with a 5 nm layer of Pt, before being examined in a FEI Nova Nanoscope 450 scanning electron microscope (SEM). Transmission Electron Microscopy (TEM) analysis and electron diffraction of the TEM grids were carried out

with a Phillips Tecnai FEG-TEM operating at 200 kV, with associated Energy-Dispersive X-ray analysis (EDX).

## RESULTS

**Precipitation in Bulk Solution.** Experiments were first conducted in bulk solution to determine the rate of transformation of ACC and its crystallisation products, where samples were analysed using TEM. Precipitation of  $\text{CaCO}_3$  in bulk solutions of concentration  $[\text{Ca}^{2+}] = [\text{CO}_3^{2-}] = 4.5 \text{ mM}$  led to the formation of ACC nanoparticles in less than 1 min and after 24 h all the precipitates were calcite (Figure 1a,b). In 2.5 mM  $\text{CaCO}_3$  solutions, ACC precipitates were detected after 15 s (Figure 1c), and calcite crystals were first observed after 5 min (Figure 1d), in agreement with our previous work<sup>29</sup> and older data in the literature.<sup>7,47</sup> Very occasionally small amounts of vaterite (ca. 0.1 %) could be observed at times up to 6 h, but after 24 h only calcite was found. At a concentration of 1.5 mM, ACC particles could be found in only half (5 out of 10) the experiments, whereas it was detected in only 3 out of 10 experiments in 1.0 mM  $\text{CaCO}_3$  solution. Only calcite was ever observed in the 1.0 and 1.5 mM solutions at precipitation times ranging from 30 min to 24 h, as confirmed with electron diffraction. No ACC or calcite were ever found in 0.5 mM solutions after 24 h (in a total of 10 experiments).

**Precipitation in Confinement.** Precipitation from metastable  $\text{CaCO}_3$  solutions confined between glass surfaces of radius  $R = 5 \text{ cm}$  in a crossed-cylinder arrangement was carried out using solution concentrations of 4.5 mM, 1.5 mM, 1.0 mM and 0.5 mM. Under conditions of  $[\text{Ca}^{2+}] = [\text{CO}_3^{2-}] = 4.5 \text{ mM}$ , the regions of surface separation  $h \geq 2.5 \text{ }\mu\text{m}$  contained non-oriented rhombohedral calcite crystals less than  $2 \text{ }\mu\text{m}$  in size after 1 day (Figure 2a). At  $h \approx 1 \text{ }\mu\text{m}$  plate-like crystals less

than 0.5  $\mu\text{m}$  in size were found (Figure 2b, which were shown to be vaterite using electron diffraction (Figure 2c). For  $h \leq 0.5 \mu\text{m}$ , only aggregates of spherical particles with morphologies consistent with ACC were observed (Figure 2d,e), and the lack of crystallinity of morphologically-similar particles was confirmed by electron diffraction (Figure 2f). These results can be compared with those of our previous study in which the glass cylinders were coated with gold and mercaptohexadecanoic acid SAMs.<sup>34</sup> Under identical solution conditions, and after the same precipitation time of 24 h, increasing amounts of ACC and less calcite was found with increasing confinement, and no vaterite was ever detected.

Looking then at lower concentrations, after a precipitation time of 24 h the precipitates in 1.5 mM solution at  $h > 10 \mu\text{m}$  were all calcite (Figure 3a,b). For  $h \approx 5 - 10 \mu\text{m}$  vaterite was found alongside particles with an ACC-like morphology (Figure 3c,d), while below  $h \approx 2.5 \mu\text{m}$  only ACC particles of diameter ca. 30-50 nm were evident (Figure 3e,f). That these particles were amorphous was confirmed by their crystallisation after 5 days in humid conditions (Figure 4). This contrasts with the data obtained in bulk solution, where ACC was only found in 50% of experiments. It is noteworthy that all the ACC, whether imaged by SEM on glass surfaces, or by TEM on Cu grids, is present as isolated particles. Interestingly, the precipitate on a TEM grid was identified as vaterite with electron diffraction (Figure 3c), where particles of similar morphology were also on the glass surface with SEM in Figure 3d.

In 1.0 mM  $\text{CaCO}_3$  solution small calcite particles were the only product after one day for  $h > 10 \mu\text{m}$  (Figure 5a, b), while for separations of 5 - 10  $\mu\text{m}$  aggregates of nanoparticles were present (Figure 5c, d), with those on the TEM grids identified as amorphous. For  $h < 2.5 \mu\text{m}$  only



nanoparticles of diameter  $< 30$  nm were found (Figure 5e,f), with similar precipitates on the TEM grid showing no crystallinity. Almost all these ACC particles were singly dispersed, with the exception of some on the TEM grid. At 0.5 mM, sparsely distributed individual nanoparticles of diameter 10-15 nm could be found on the TEM grids, where these were too small to analyse with selected-area electron diffraction (Figure 6). Again, these data strongly suggest a significant influence of physical confinement on crystallisation pathways, where no precipitates were ever observed in bulk solutions of concentration 0.5 mM.

## **DISCUSSION**

These experiments reveal a number of interesting phenomena. The first striking observation is the persistence of ACC in confined volumes. While ACC was only very occasionally detected in the bulk solution at concentrations of 1-1.5 mM, it was present in confinement for at least one day at surface separations in the range 2.5 – 10  $\mu\text{m}$ . At 0.5 mM the identity of the particles that were observed in confinement could not be confirmed (due to their small numbers), but their appearance is consistent with ACC. Notably, such particles were never found in bulk solution, nor in equally confined solutions of pure  $\text{Na}_2\text{CO}_3$  or pure  $\text{CaCl}_2$ . The stabilisation that ACC experiences in confinement therefore enables us to detect this phase at solution concentrations where it is extremely challenging to observe in bulk. Further, the detection of ACC from 0.5 mM solutions also provides further validation of the results of Kellermeier et al.,<sup>46</sup> who used a titration study to infer that the solubility of ACC is considerably lower than previously thought.

We have also considered the possibility that ACC can precipitate in confinement under conditions where it would not form in bulk solution – that is, it is stabilised below the bulk solubility limit by

solid surfaces. This situation would be analogous to capillary condensation of a liquid from vapour below the bulk melting point of the liquid, where the bulk liquid is unstable, but can be stabilised by being confined between solid surfaces.<sup>48-50</sup> Such capillary condensates are metastable with respect to crystallisation, but not towards evaporation. They are stabilised by the solid surface because the interfacial free energy between the liquid condensate and the solid substrate is lower than between the vapour and the solid substrate. In the present case, the ACC would be metastable towards crystallisation, but stable towards dissolution in the aqueous phase. The requirements for ACC to “capillary condense” would be that the surface free energy of the solid-ACC interface is lower than that of the solid-solution interface, or equivalently, that the contact angle of the ACC on the substrate is clearly lower than 90°. From electron micrographs (Figure 7) it is apparent that the ACC particles hardly make contact with the glass, or the polymer coating on the TEM grid. The contact angle of ACC on the surfaces in our system appears to be in the range 90-180°, and we therefore believe that we can confidently discount “capillary condensation” of ACC as an explanation for its occurrence in the confined system.

Importantly, significant differences in the degree of aggregation of the ACC particles were observed according to the degree of confinement. The spherical ACC particles present after 1 day for  $h < 0.5 \mu\text{m}$  at 4.5 mM had all aggregated, but after 1 day for  $h < 2.5 \mu\text{m}$  at 1 mM and 1.5 mM they were almost exclusively isolated particles. By comparison, in bulk solution at 2 mM the ACC was mainly single particles after 15 s, but had clustered considerably after 2 min, when calcite crystals were already present. Similarly, our previous study of ACC precipitation in bulk at concentrations of 2.5-5 mM showed significant aggregation of the ACC 5 min after precipitation.<sup>51</sup> This strongly suggests that the degree of aggregation plays a key role in defining the lifetime of

ACC. Although the SEM images were by necessity obtained after drying of the samples, it is extremely unlikely that this would have led to dispersal of aggregated particles. Indeed, drying of nanoparticles suspended in a solvent is frequently used as a means of assembling dispersed particles.<sup>52</sup>

On the assumption that one nucleation event for each ACC particle or aggregate of ACC particles is required for conversion to calcite it is clear that – if the particles are fixed in position such that they do not interact with each other – the total number of nucleation events to convert all of the ACC to calcite is much larger for highly dispersed particles. This argument also highlights a key difference between confined systems and bulk solutions. Precipitates formed in confined volumes are typically fixed in position (being located on a surface) or have limited freedom of movement, and thus only experience their local environments. This is in stark contrast to bulk solutions, where diffusion and convection processes ensure that the formation of a nucleus of a more stable polymorph rapidly destabilises the original population of metastable particles. Such a mechanism was postulated in connection with the stabilisation of bassanite with regard to conversion to gypsum.<sup>39</sup> However, we were unable to conclusively determine whether a change in aggregation behaviour with degree of confinement in the case of ACP,<sup>41</sup> as after 3 days all amorphous calcium phosphate at surface separations  $h > 0.5 \mu\text{m}$  had transformed to octacalcium phosphate or hydroxyapatite, and no observations were made for shorter precipitation times.

Finally, our experiments reveal the presence of vaterite under certain solution concentrations and confinement conditions. Notably, no vaterite was detected in our previous experiments with 4.5 mM solutions and SAM-functionalised glasses. That 4.5 mM solutions and uncoated glass yielded

vaterite can therefore be attributed to the substrate surface chemistry, where MHA surfaces favour the nucleation of calcite.<sup>45</sup> Indeed, that subtle changes in surface chemistry can lead to vaterite/polymorph selectivity has previously been observed for the precipitation of calcium carbonate in the pores of track-etched membranes.<sup>53</sup> In addition, vaterite as an intermediate has previously been found in less well-defined confined systems such as a gelatin matrix<sup>54</sup> or self-assembled lecithin structures.<sup>55</sup> Our current experiments also reveal that vaterite was present for up to three days at concentrations of 1.5 mM and separations as large as 5-10  $\mu\text{m}$ , but undetectable in bulk solution at these concentrations. This behaviour is consistent again with our studies of calcium sulfate and calcium phosphate precipitation in the crossed-cylinder apparatus, where the key metastable crystalline phases bassanite and octacalcium phosphate were observed at intermediate levels of confinement.<sup>39,41</sup>

## CONCLUSIONS

These results highlight the utility of confinement effects in allowing the observation of intermediate or precursor phases that are only transiently stable in bulk solutions. ACC particles can be imaged under conditions where the low concentration or short lifetime preclude their observation in bulk solution. Notably, we also observe vaterite as an intermediate polymorph under solution conditions where negligible is found in bulk solution, suggesting that confinement can also modify the pathway by which crystallisation occurs. Our results show how surface chemistry and confinement act together to control crystallisation and bring our studies of calcium carbonate precipitation in confinement in line with the crystallisation pathways previously observed for calcium sulfate and calcium phosphate in restricted volumes. Finally, our data support the case for the restricted mobility and hindered aggregation as an important stabilisation

mechanism of metastable phases in confinement. That confinement can be used to stabilise ACC – or indeed alternative amorphous precursor phases – in the absence of additives or capping agents which may interfere with subsequent processing - promises a potential route for stabilising and controlling the crystallisation of amorphous precursor phases for practical applications.

## ACKNOWLEDGEMENTS

This work was supported by an Engineering and Physical Sciences Research Council (EPSRC) Leadership Fellowship (F.C.M. and Y.W.W., EP/H005374/1) and an EPSRC Platform Grant (F.C.M and H.K.C., EP/N002423/1).

## References

- (1) De Yoreo, J. J.; Gilbert, P. U. P. A.; Sommerdijk, N. A. J. M.; Penn, R. L.; Whitlam, S.; Joester, D.; Zhang, H.; Rimer, J. D.; Navrotsky, A.; Banfield, J. F.; Wallace, A. F.; Michel, F. M.; Meldrum, F. C.; Coelfen, H.; Dove, P. M., *Science* **2015**, 349.
- (2) Gal, A.; Weiner, S.; Addadi, L., *CrystEngComm* **2015**, 17, 2606-2615.
- (3) Gebauer, D.; Völkel, A.; Cölfen, H., *Science* **2008**, 322, 1819-1822.
- (4) Gebauer, D.; Kellermeier, M.; Gale, J. D.; Bergström, L.; Cölfen, H., *Chem. Soc. Rev.* **2014**, 43, 2348-2371.
- (5) Neumann, M.; Epple, M., *Eur. J. Inorg. Chem.* **2007**, 1953–1957.
- (6) Gebauer, D.; Gunawidjaja, P. N.; Ko, J. Y. P.; Bacsik, Z.; Aziz, B.; Liu, L.; Hu, Y.; Bergström, L.; Tai, C.-W.; Sham, T.-K.; Edén, M.; Hedin, N., *Angew. Chem. Int. Ed.* **2010**, 49, 8889 –8891
- (7) Zou, Z.; Bertinetti, L.; Politi, Y.; Jensen, A. C. S.; Weiner, W.; Addadi, L.; Fratzl, P.; Habraken, W. J. E. M., *Chem. Mater.* **2015**, 27, 4237-4246.
- (8) Farhadi-Khouzani, M.; Chevrier, D. M.; Zhang, P.; Hedin, N.; Gebauer, D., *Angew. Chem. Int. Ed.* **2016**, 55, 1-5.
- (9) Lam, R. S. K.; Charnock, J. M.; Lennie, A.; Meldrum, F. C., *CrystEngComm* **2007**, 9, 1226-1236.
- (10) Ihli, J.; Wong, W. C.; Noel, E. H.; Kim, Y.-Y.; Kulak, A. N.; Christenson, H. K.; Duer, M. J.; Meldrum, F. C., *Nat. Commun.* **2014**, 5, 3169.
- (11) Schmidt, M. P.; Ilott, A. J.; Phillips, B. L.; Reeder, R. J., *Cryst. Growth Des.* **2014**, 14, 938-951.

- (12) Goodwin, A. L.; Michel, F. M.; Phillips, B. L.; Keen, D. A.; Dove, M. T.; Reeder, R. J., *Chem. Mater.* **2010**, *22*, 3197-3205.
- (13) Rieger, J.; Frechen, T.; Cox, G.; Heckmann, W.; Schmidt, C.; Thieme, J., *Faraday Discuss.* **2007**, *136*, 265-277.
- (14) Wallace, A. F.; Hedges, L. O.; Fernandez-Martinez, A.; Raitteri, P.; Gale, J. D.; Waychunas, G. A.; Whitelam, S.; Banfield, J. F.; De Yoreo, J. J., *Science* **2013**, *341*, 885-889.
- (15) Zou, Z.; Habraken, W. J. E. M.; Bertinetti, L.; Politi, Y.; Gal, A.; Weiner, S.; Addadi, L.; Fratzl, P., *Adv. Mater. Interfaces* **2016**, *4*, 1600076.
- (16) Cantaert, B.; Kuo, D.; Matsumura, S.; Nishimura, T.; Sakamoto, T.; Kato, T., *ChemPlusChem* **2017**, *82*, 107-120.
- (17) Lee, K.; Wagermaier, W.; Masic, A.; Kommareddy, K. P.; Bennet, M.; Manjubala, I.; Lee, S. W.; Park, S. B.; Colfen, H.; Fratzl, P., *Nat. Commun.* **2012**, *3*, 7.
- (18) Barhoum, A.; Van Lokeren, L.; Rahier, H.; Dufresne, A.; Van Assche, G., *J. Mater. Sci.* **2015**, *50*, 7908-7918.
- (19) Yao, H. B.; Ge, J.; Mao, L. B.; Yan, Y. X.; Yu, S. H., *Adv. Mater.* **2014**, *26*, 163-188.
- (20) Aizenberg, J.; Muller, D. A.; Grazul, J. L.; Hamann, D. R., *Science* **2003**, *299*, 1205-1208.
- (21) Zhao, Y.; Luo, Z.; Li, M. H.; Qu, Q. Y.; Ma, X.; Yu, S. H.; Zhao, Y. L., *Angew. Chem. Int. Ed.* **2015**, *54*, 919-922.
- (22) Qi, C.; Zhu, Y. J.; Lu, B. Q.; Zhao, X. Y.; Zhao, J.; Chen, F.; Wu, J., *Small* **2014**, *10*, 2047-2056.
- (23) Meiron, O. E.; Bar-David, E.; Aflalo, E. D.; Shechter, A.; Stepensky, D.; Berman, A.; Sagi, A., *J. Bone Miner. Res.* **2011**, *26*, 364-372.
- (24) Ping, H.; Xie, H.; Wan, Y. M.; Zhang, Z. X.; Zhang, J.; Xiang, M. Y.; Xie, J. J.; Wang, H.; Wang, W. M.; Fu, Z. Y., *J. Mater. Chem. B* **2016**, *4*, 880-886.
- (25) Addadi, L.; Raz, R.; Weiner, S., *Adv. Mater.* **2003**, *15*, 959-970.
- (26) Ihli, J.; Kim, Y.-Y.; Noel, E. H.; Meldrum, F. C., *Adv. Funct. Mater.* **2013**, *23*, 1575-1585.
- (27) Kababya, S.; Gal, A.; Kahil, K.; Weiner, S.; Addadi, L.; Schmidt, A., *J. Am. Chem. Soc* **2015**, *137*, 990-998.
- (28) Schenk, A. S.; Cantaert, B.; Kim, Y.-Y.; Li, Y.; Read, E. S.; Semsarilar, M.; Armes, S. P.; Meldrum, F. C., *Chem. Mater.* **2014**, *26*, 2703-2711.
- (29) Wang, Y. W.; Kim, Y. Y.; Stephens, C. J.; Meldrum, F. C.; Christenson, H. K., *Cryst. Growth Des.* **2012**, *12*, 1212-1217.
- (30) Pouget, E. M.; Bomans, P. H. H.; Goos, J. A. C. M.; Frederik, P. M.; de With, G.; Sommerdijk, N. A. J. M., *Science* **2009**, *323*, 1455-1458.
- (31) Lee, J. R. I.; Han, T. Y. J.; Willey, T. M.; Wang, D.; Meulenberg, R. W.; Nilsson, J.; Dove, P. M.; Terminello, L. J.; van Buuren, T.; De Yoreo, J. J., *J. Am. Chem. Soc* **2007**, *129*, 10370-10381.
- (32) Loste, E.; Park, R. J.; Warren, J.; Meldrum, F. C., *Adv. Funct. Mater.* **2004**, *14*, 1211-1220.
- (33) Kim, Y.-Y.; Hetherington, N. B. J.; Noel, E. H.; Kroeger, R.; Charnock, J. M.; Christenson, H. K.; Meldrum, F. C., *Angew. Chem. Int. Ed.* **2011**, *50*, 12572-12577.
- (34) Stephens, C. J.; Ladden, S. F.; Meldrum, F. C.; Christenson, H. K., *Adv. Funct. Mater.* **2010**, *20*, 2108-2115.
- (35) Tester, C. C.; Whittaker, M. L.; Joester, D., *Chem. Commun.* **2014**, *50*, 5619-5622.
- (36) Stephens, C. J.; Kim, Y.-Y.; Evans, S. D.; Meldrum, F. C.; Christenson, H. K., *J. Am. Chem. Soc* **2011**, *133*, 5210-5213.

- (37) Tester, C. C.; Brock, R. E.; Wu, C.-H.; Krejci, M. R.; Weigand, S.; Joester, D., *CrystEngComm* **2011**, 13, 3975-3978.
- (38) Nielsen, M. H.; Shaul Aloni, S.; De Yoreo, J. J., *Science* **2014**, 345, 1158-1162.
- (39) Wang, Y.-W.; Christenson, H. K.; Meldrum, F. C., *Adv. Funct. Mater.* **2013**, 23, 5615–5623.
- (40) Ihli, J.; Wang, Y. W.; Cantaert, B.; Kim, Y. Y.; Green, D. C.; Bomans, P. H. H.; Sommerdijk, N. A. J. M.; Meldrum, F. C., *Chem. Mater.* **2015**, 27, 3999-4007.
- (41) Wang, Y.-W.; Christenson, H. K.; Meldrum, F. C., *Chem. Mater.* **2014**, 26, 5830-5838.
- (42) Cantaert, B.; Beniash, E.; Meldrum, F. C., *Chem. Eur. J.* **2013**, 19, 14918-14924.
- (43) Anduix-Canto, C.; Kim, Y.-Y.; Wang, Y.; Kulak, A.; Meldrum, F. C.; Christenson, H. K., *Cryst. Growth. Des.* **2016**, 16, 5403-5411.
- (44) Jiang, Q.; Ward, M. D., *Chem. Soc. Rev.* **2014**, 43, 2066-2079.
- (45) Aizenberg, J.; Black, A. J.; Whitesides, G. M., *J. Am. Chem. Soc.* **1999**, 121, 4500-4509.
- (46) Kellermeier, M.; Picker, A.; Kempter, A.; Cölfen, H.; Gebauer, D., *Adv. Mater.* **2014**, 26, 752–757.
- (47) Brecevic, L.; Nielsen, A. E., *J. Cryst. Growth* **1989**, 98, 504-510.
- (48) Nowak, D.; Christenson, H. K., *Langmuir* **2009**, 25, 9908-9912.
- (49) Nowak, D.; Heuberger, M.; Zäch, M.; Christenson, H. K., *J. Chem. Phys.* **2008**, 129, 154509.
- (50) Christenson, H. K., *Phys. Rev. Lett.* **1995**, 74, 4675-4678.
- (51) Wang, Y.; Stephens, C. J.; Kim, Y.-Y.; Meldrum, F. C.; Christenson, H. K., *Cryst. Growth. Des.* **2012**, 12, 1212-1217.
- (52) Bigoni, T. P.; Lin, X.-M.; Nguyen, T. T.; Corwini, E. I.; Witten, T. A.; Jaeger, H. M., *Nat. Mater.* **2006**, 5, 265-270.
- (53) Schenk, A. S.; Albarracin, E. J.; Kim, Y. Y.; Ihli, J.; Meldrum, F. C., *Chem. Commun.* **2014**, 50, 4729-4732.
- (54) Zhan, J.; Lin, H.-P.; Mou, C.-Y., *Adv. Mater.* **2003**, 15, 621-623.
- (55) Beato, C.; Fernández, M. S.; Fermani, S.; Reggi, M.; Neira-Carrillo, A.; Rao, A.; Falinib, G.; Arias, J. L., *CrystEngComm* **17**, 5953-5961.

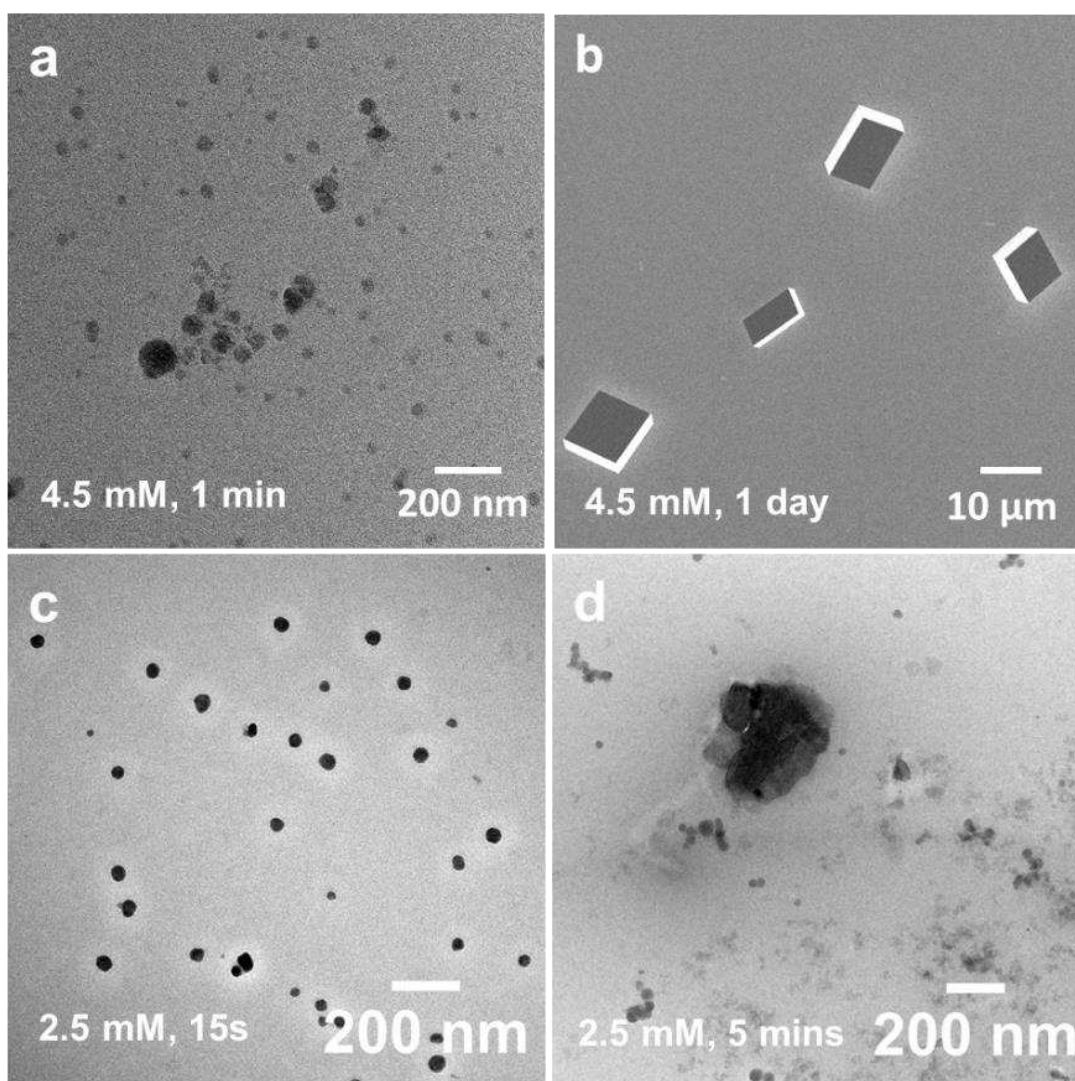


**Figure 1.** Precipitates formed in metastable bulk CaCO<sub>3</sub> solutions. At 4.5 mM the precipitates were (a) ACC nanoparticles after 1 min, and (b) calcite after 1 day. (c) At 2.5 mM after 15 s all precipitates were consistently (in 5 samples) ACC particles. (d) Calcite crystals were first observed after 5 min.



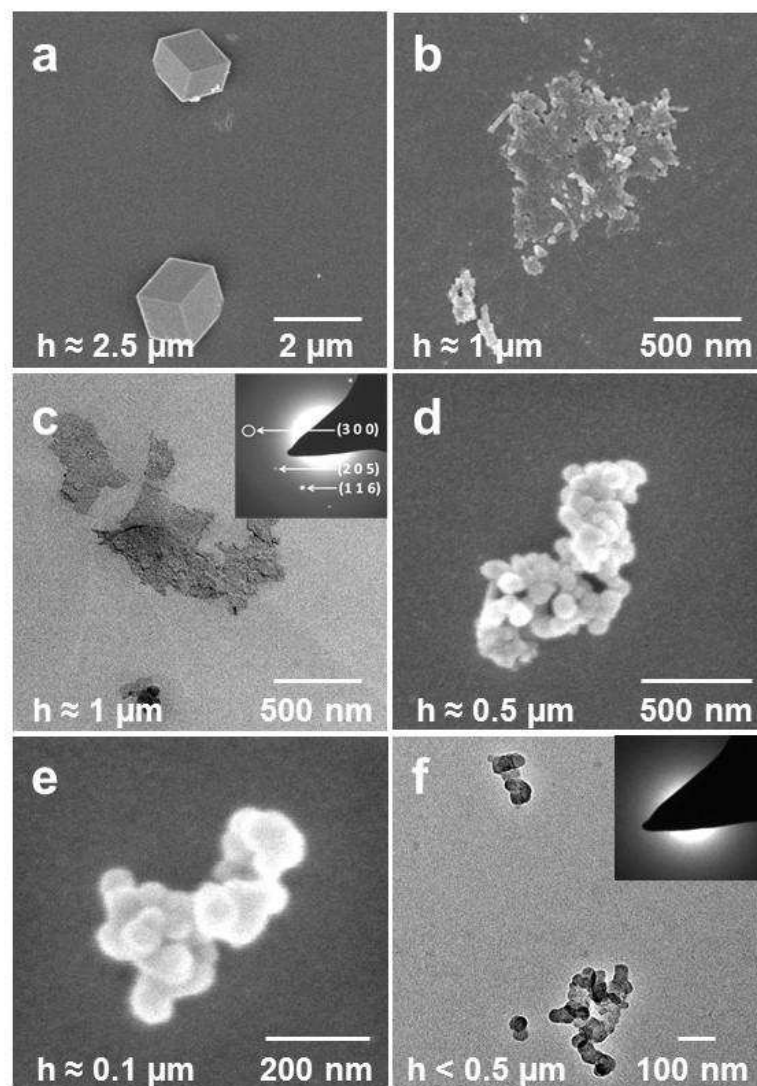


**Figure 2.** Calcium carbonate particles formed in confinement from solutions of concentration  $[\text{Ca}^{2+}] = [\text{CO}_3^{2-}] = 4.5 \text{ mM}$  after 1 day at the following surface separations. (a)  $h \approx 2.5 \mu\text{m}$ , where all precipitates were rhombohedral calcite, less than  $2 \mu\text{m}$  in size. (b, c)  $h \approx 1 \mu\text{m}$ , where plate-like crystals of vaterite were observed, less than  $0.5 \mu\text{m}$  in size, as confirmed by electron diffraction (inset, c). (d, e and f) Only ACC was found (lack of diffraction pattern in inset) when  $h < 0.5 \mu\text{m}$ . (a, b, d, e): SEM images and (c, f) TEM images.

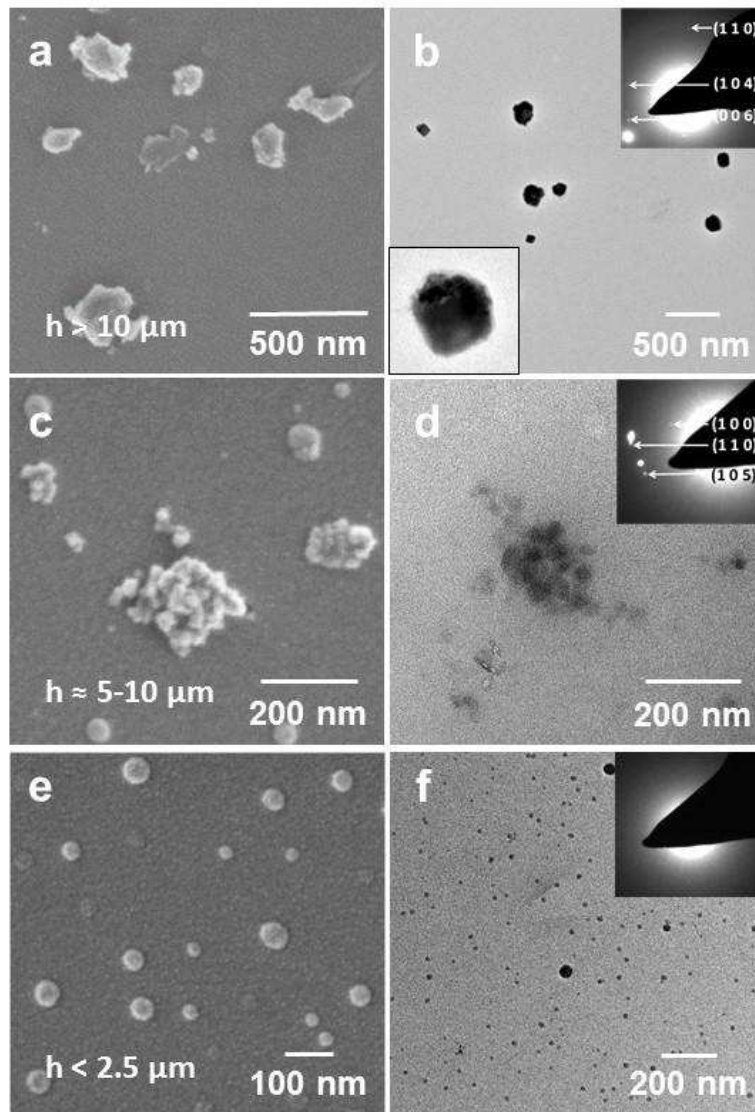


**Figure 3.**  $\text{CaCO}_3$  precipitates formed in solutions of concentration  $[\text{Ca}^{2+}] = [\text{CO}_3^{2-}] = 1.5 \text{ mM}$  at various surface separations after 1 day. (a and b)  $h > 10 \mu\text{m}$ , where all the precipitates were calcite. (c and d) In the region of  $5\text{-}10 \mu\text{m}$ , vaterite could be observed and was stable for up to 3 days in confinement. (e and f) Only single ACC particles, less than  $50 \text{ nm}$  in diameter were found for  $h < 2.5 \mu\text{m}$ . (a, c, e) SEM images, (b, d, f) TEM images with electron diffraction patterns.

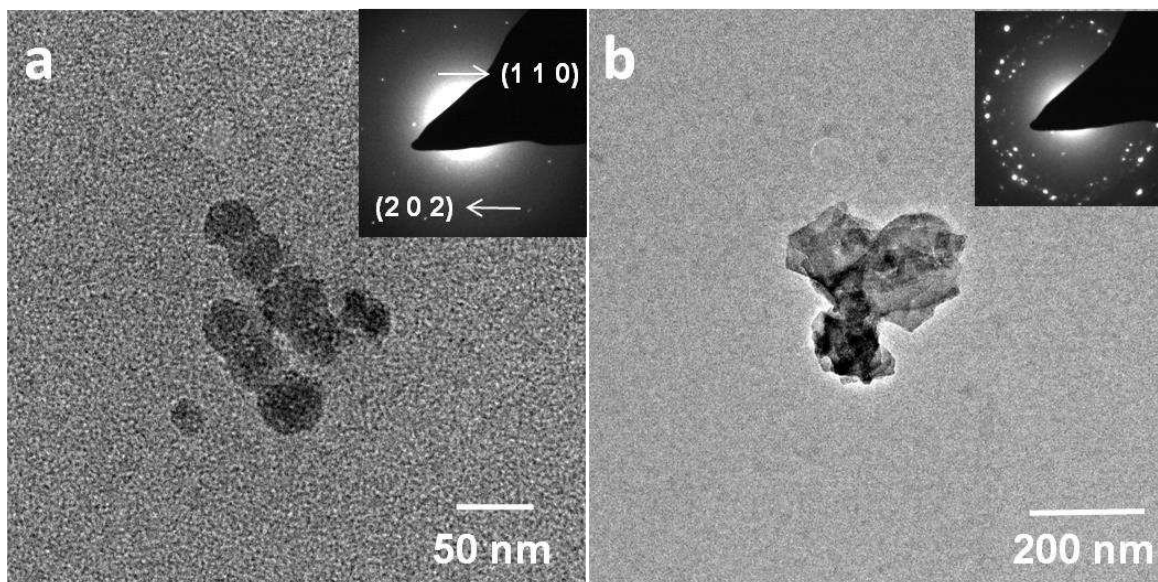


**Figure 4.** Images of ACC particles extracted from 1.5 mM  $\text{CaCO}_3$  after 1 day in confinement at  $h \approx 2.5 \mu\text{m}$  and left in a humid atmosphere for 5 days. The sharp rings and spots, rather than diffuse rings, in the electron diffraction patterns accompanying (insets) the TEM images shows that the ACC has crystallised.

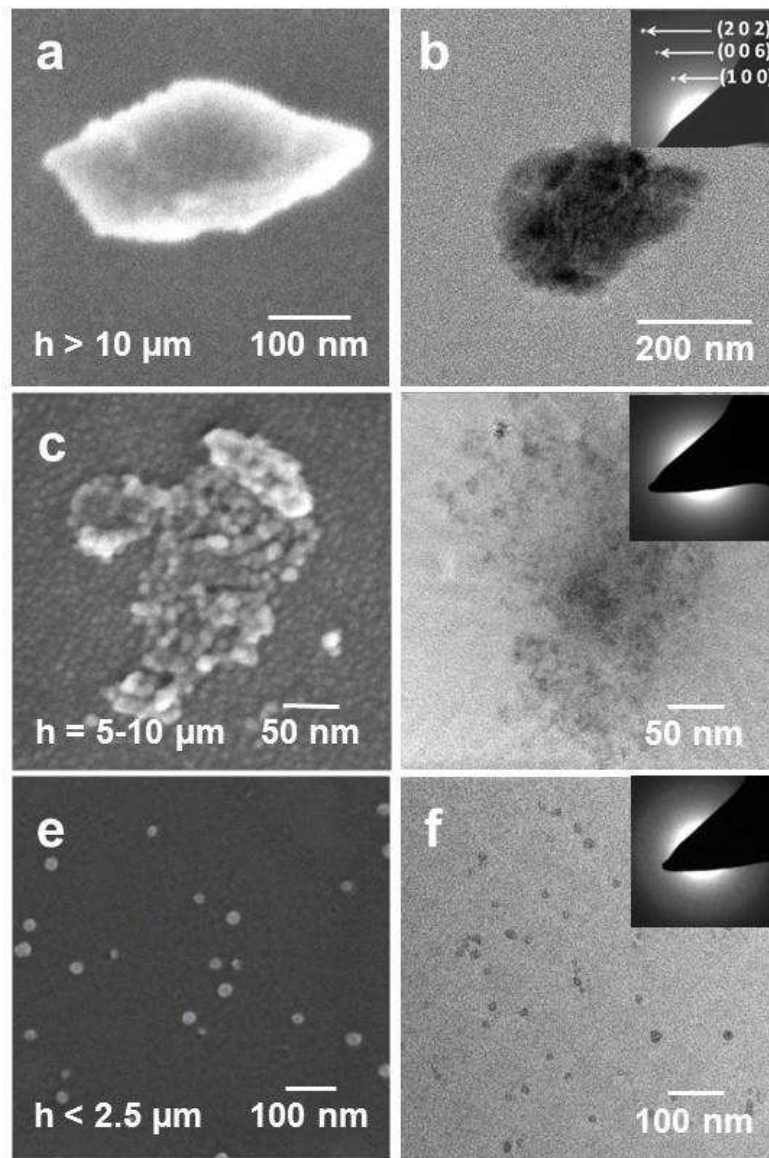


**Figure 5.**  $\text{CaCO}_3$  precipitates from solutions of concentration  $[\text{Ca}^{2+}] = [\text{CO}_3^{2-}] = 1 \text{ mM}$  in confinement at various surface separations after 1 day. (a, b)  $h > 10 \mu\text{m}$ , all the precipitates were calcite. (c,d) For  $h = 5\text{-}10 \mu\text{m}$ , clusters of nanoparticles were found. (e and f) Mainly single ACC particles, less than 30 nm in the diameter, can be seen when  $h < 2.5 \mu\text{m}$ . (a, c, e) SEM images, (b, d, f) TEM images with electron diffraction patterns.

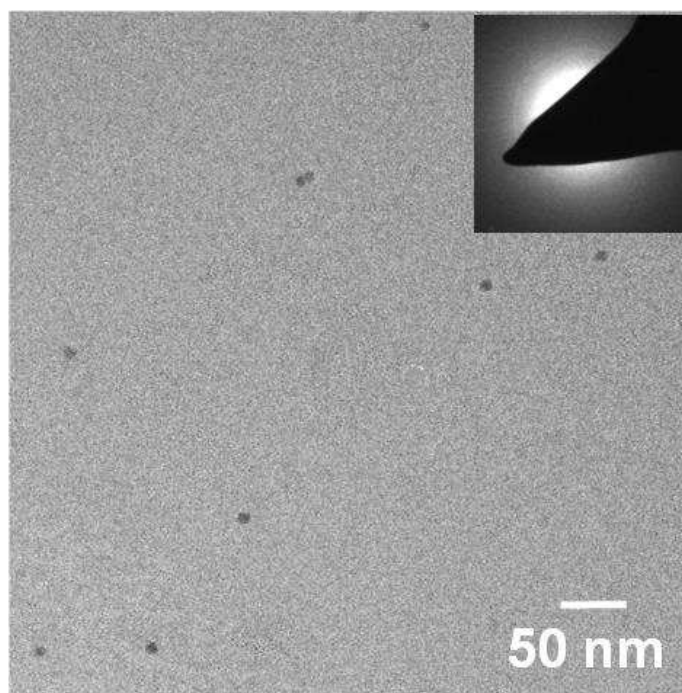


**Figure 6.** Particles precipitates from solutions of concentration  $[\text{Ca}^{2+}] = [\text{CO}_3^{2-}] = 0.5 \text{ mM}$  for  $h < 0.5 \text{ }\mu\text{m}$ , after 24 h. Too small ( $< 10 \text{ nm}$ ) to analyse by electron diffraction, we cannot conclusively prove that they are ACC. However, such particles were not seen at larger surface separations, nor in solutions of pure  $\text{CaCl}_2$  or pure  $\text{Na}_2\text{CO}_3$ .

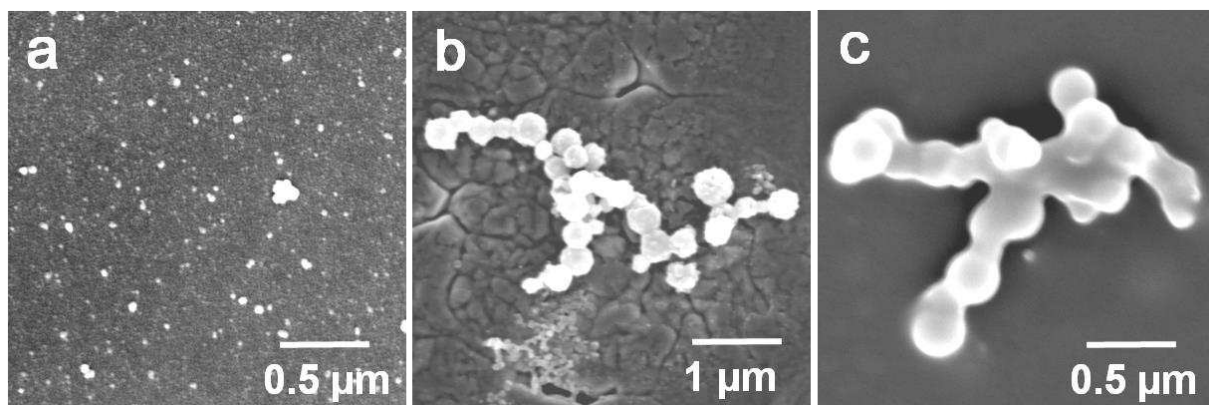


**Figure 7.** The morphology of ACC precipitated on different surfaces. (a) On bare glass slide, (b) on a bare copper grid (without membrane) and (c) on a copper TEM grid (with membrane). In all cases the particles appear to barely make contact with the surfaces, showing that the effective contact angle is much larger than  $90^\circ$ .

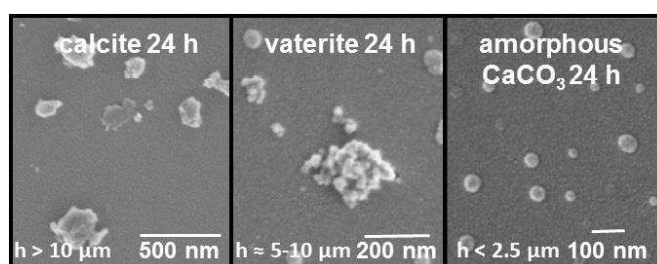
**For Table of Contents Use Only**

**Using Confinement to Study the Crystallisation Pathway of Calcium Carbonate**

Yunwei Wang<sup>1</sup>, Muling Zeng<sup>2</sup>, Fiona C. Meldrum<sup>1\*</sup> and Hugo K. Christenson<sup>2\*</sup>

<sup>1</sup>School of Chemistry, <sup>2</sup>School of Physics and Astronomy, University of Leeds,

Leeds, LS2 9JT, UK.



**Synopsis**

In confinement amorphous calcium carbonate (ACC) is observable at concentrations where it is almost undetectable in bulk, and it persists for much longer, which we attribute to decreased aggregation. Confined ACC transforms to calcite via vaterite at concentrations where direct transformation to calcite occurs in bulk. This shows the utility of confinement for the stabilisation and detection of metastable phases.